Atomic scale observation of threading dislocations in α-Ga_2O_3

Cite as: AIP Advances 14, 115018 (2024); doi: 10.1063/5.0235005
Submitted: 24 September 2024 • Accepted: 28 October 2024 •
Published Online: 14 November 2024

Ross Mullen,[1] Joseph W. Roberts,[2] Paul R. Chalker,[2] Rachel A. Oliver,[3] Ben Hourahine,[1] and Fabien C. P. Massabuau[1,a)]

AFFILIATIONS

[1] Department of Physics, SUPA, University of Strathclyde, Glasgow G4 0NG, United Kingdom
[2] School of Engineering, University of Liverpool, Liverpool L69 3GH, United Kingdom
[3] Department of Material Science and Metallurgy, University of Cambridge, Cambridge CB3 0FS, United Kingdom

[a)] **Author to whom correspondence should be addressed:** f.massabuau@strath.ac.uk

ABSTRACT

This study presents a statistically significant investigation of threading dislocations in α-Ga_2O_3 using high-resolution transmission electron microscopy. All the dislocations, observed end on, exhibit a projected Burgers vector $\mathbf{b_e} = \frac{1}{3}\langle 1\bar{1}00\rangle$, with data revealing that the dislocations fall into three categories: perfect mixed ($\mathbf{b} = \frac{1}{3}\langle 1\bar{1}01\rangle$) dislocations and edge ($\mathbf{b} = \langle 1\bar{1}00\rangle$ and $\mathbf{b} = \frac{1}{3}\langle 11\bar{2}0\rangle$) dislocations, which dissociate into combinations of $\mathbf{b} = \frac{1}{3}\langle 1\bar{1}00\rangle$ partials. High-resolution analysis of the core region of the dislocations identifies that all the dislocations exhibit a similar 5-atom core, when looking at the cation sites. This is the first investigation of its kind in this material system, which will inform future work to, for example, understand the electronic properties of dislocations in α-Ga_2O_3 and other epitaxial corundum-structured materials.

Gallium oxide (Ga_2O_3) has recently emerged as the leading candidate for future power electronic and deep ultraviolet optoelectronic applications.[1,2] This compound is highly polymorphic, with five known phases labeled α, β, κ, δ, and γ.[3–5] Research to date has been driven by the monoclinic β-phase of Ga_2O_3 as the thermodynamic stability of this phase implies that it can be produced in bulk.[6] On the other hand, the rhombohedral corundum-like α-phase of Ga_2O_3 is rapidly gaining interest[7] due to its bandgap energy of ~5.1–5.6 eV (the widest bandgap among all Ga_2O_3 phases)[8–10] and its isomorphism with a range of semiconductor sesquioxides.[11] Despite its metastability, α-Ga_2O_3 can now be deposited on the isomorphic, inexpensive, and widely available α-Al_2O_3 (sapphire) substrate using most common deposition techniques.[12] A drawback of heteroepitaxy is that the deposition of the film on a lattice-mismatched substrate will almost unavoidably generate dislocations to accommodate that strain. This has been widely reported in previous generations of semiconductors,[13,14] and early reports on α-Ga_2O_3 show that this compound is no exception. In the absence of dislocation mitigation strategies, epitaxial α-Ga_2O_3 films typically exhibit threading dislocation densities of the order of 10^{10} cm^{-2}.[15–18] Densities down to 10^8 cm^{-2} were achieved using $(Al_xGa_{1-x})_2O_3$ graded buffer layers,[19] epitaxial lateral overgrowth,[16] or rapid low temperature growth of thick films,[20] and the combination of the two latter methods results in a further decrease in density down to ~10^7 cm^{-2}.[20] Notwithstanding these advances, the reported dislocation densities for α-Ga_2O_3 on α-Al_2O_3 are too high to be ignored.

The impact of dislocations on the properties of α-Ga_2O_3 materials and devices has been poorly understood to date. In the III–V semiconductor systems, dislocations have been associated with reduced light emission,[21] reduced device reliability,[22] or increased leakage current.[23] In β-Ga_2O_3, where these defects are less studied, dislocations have been related to reverse leakage current,[24] curbed breakdown voltage,[25] and reduced luminescence.[26] In α-Ga_2O_3, Takane *et al.* linked dislocation density to reduced electron mobility and calculated that dislocation density ≤10^7–10^8 cm^{-2} was required to nullify their impact.[27]

However, while the general expectation is that they have a negative influence on material properties, not all dislocations are identical nor have deleterious effects. Reports on GaN indicate that only pure screw dislocations affect leakage current, unlike edge and mixed dislocations.[28–30] Moreover, dislocations can enable material engineering breakthroughs, for example acting as porosification

channels for novel optical devices.[31] Similarly to III-nitrides, a better understanding of dislocations in α-Ga_2O_3 will underpin targeted material and device fabrication strategies. This will result in efficient and reliable devices performing to the theoretical promises of the materials. The journey to build this understanding commences by observing and identifying the dislocations present in the material.

Earlier reports used transmission electron microscopy (TEM) and **g.b** analysis[32] to observe dislocations in α-Ga_2O_3 and identify their character (edge, screw, and mixed).[15,17,19,20] As threading dislocations have a line direction along [0001] for epitaxially grown materials, **g** conditions such as $1\bar{1}00$ or $11\bar{2}0$ would highlight the dislocation's edge component, while **g** conditions parallel to 0001 are used to visualize the screw component. The literature so far concluded that threading dislocations in α-Ga_2O_3 films are dominantly edge-type,[15,17,20] with few reports of dislocations with screw-component.[19,33] Ma *et al.* and Takane *et al.* used x-ray diffraction to calculate the density of dislocations from the broadening of the reflection, with similar conclusions as the TEM approach.[18,34] This led to the, perhaps hasty, conclusion that dislocations are perfect with Burgers vector $\mathbf{b} = \frac{1}{3}\langle 11\bar{2}0\rangle$. These conclusions were, however, not informed by dislocation energy theory. Since dislocation energy is proportional to $\mathbf{b}^2$ and α-Ga_2O_3 has a particularly large unit cell (a = 4.9825 Å; c = 13.433 Å[35]), we can expect that perfect dislocations are likely to be unstable. Instead, we could reasonably expect dislocations to dissociate into partials to reduce their overall energy. Dislocation dissociation has been routinely observed in nitrides,[36–41] as well as in the isomorphic α-Al_2O_3.[42–44] While a result of this nature in α-Ga_2O_3 would not trigger a fundamental reconsideration of previous observations, a more accurate understanding of the type of dislocations present in the material is imperative to grasp their properties and to develop more effective mitigation routes. In the present study, we employ aberration-corrected high-resolution scanning transmission electron microscopy (STEM) to elucidate the nature of threading dislocations in α-Ga_2O_3 and provide the first atomic scale observation of their core structure.

An α-Ga_2O_3 film with a thickness of ~250 nm was grown on a *c*-plane sapphire substrate by plasma enhanced atomic layer deposition using an Oxford Instruments OpAL reactor at a temperature of 250 °C. A full description of the growth process can be found in Ref. 45. From previous investigations,[45,46] it is known that under these growth conditions, the resulting α-Ga_2O_3 film is grown epitaxially on the α-Al_2O_3 substrate with $[0001]_{Ga_2O_3} \| [0001]_{Al_2O_3}$ and $[11\bar{2}0]_{Ga_2O_3} \| [11\bar{2}0]_{Al_2O_3}$, and with the film consisting dominantly of α-Ga_2O_3 columns, with amorphous and κ-Ga_2O_3 inclusions located between the columns.[46]

The sample was prepared for plan-view STEM imaging using the standard mechanical polishing method followed by Ar^+ ion milling at 5 kV and cleaning from 1 kV down to 0.1 kV.[32] The sample was observed in plan-view using an FEI Titan3 aberration-corrected STEM operated at 300 kV in high-angle annular dark-field STEM (HAADF-STEM) mode. The dislocations were viewed end on—i.e., along the [0001] zone-axis—thereby allowing the identification of the core structure. Strain mapping was obtained using geometrical phase analysis.[47]

Figure 1 presents an overview of the sample observed by HAADF-STEM in plan-view geometry. The contrast in HAADF-STEM images is dominated by Rutherford scattering, i.e., proportional to Z^2, with residual contrast provided by strain and misorientation effects. As a result, the atomic scale images shown here along [0001] will be dominated by the projection of Ga (Z = 31) atomic columns rather than O (Z = 8) atomic columns. A crystal structure overlay in the inset clearly highlights the correspondence of the atoms in HAADF-STEM with Ga atomic columns.

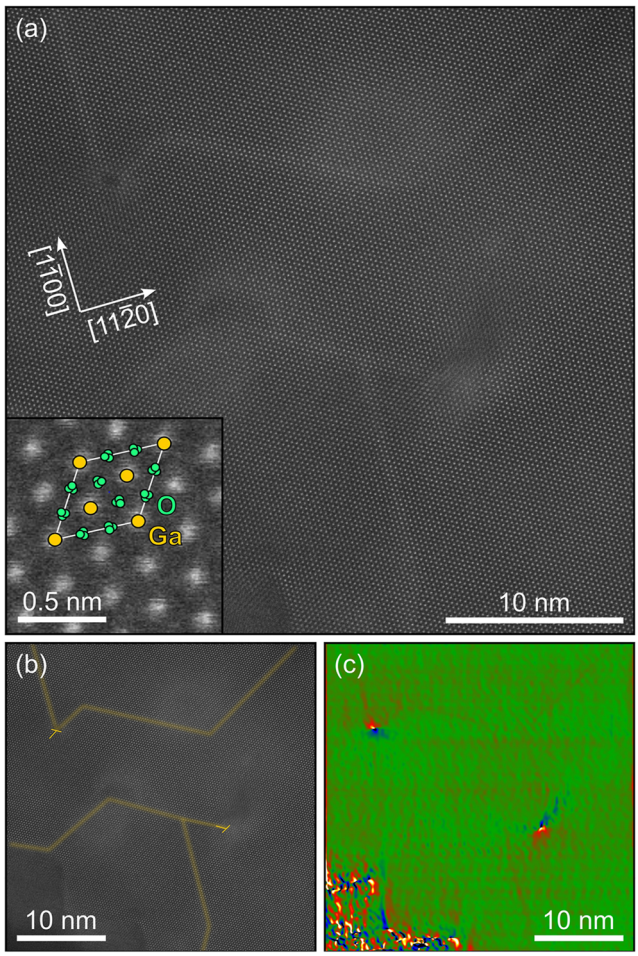

FIG. 1. (a) Raw HAADF-STEM image with a unit cell model overlay in the inset. (b) The same image highlighting the position and orientation of white lines and dislocations and (c) the corresponding strain map ϵ_{xx} along $[11\bar{2}0]$ highlighting the strain dipole at dislocations and faint strain contrast linked to the white lines.

This image can be seen to contain two threading dislocations. The presence of threading dislocations observed end on is hinted at by the local blurry contrast in HAADF-STEM [Fig. 1(a)] and by the tensile–compressive strain dipole in the strain map [Fig. 1(c)] resulting from the local distortion of the crystal lattice in the vicinity of the dislocation—more detailed analysis of the Burgers vector and core structure is presented in the following paragraphs. Using the images with widest field of view, we calculate that the film contains a threading dislocation density of $\sim 5 \times 10^{10}$ cm^{-2}, which is slightly higher compared to other reported values,[15–18] but not overly so, given that here we investigate a comparatively thinner film.

The raw, unfiltered HAADF-STEM image [Fig. 1(a)] also reveals the presence of a high density of white lines throughout the

material—these are highlighted in Fig. 1(b) for better clarity. These white lines are observed running along the $\langle 1\bar{1}00\rangle$ directions, and assuming these are the projection of a planar feature parallel to [0001], then these are contained in the $\{11\bar{2}0\}$ planes. These lines are visible in the raw HAADF-STEM images but not in the average background subtraction filter (ABSF) filtered images and exhibit a very faint contrast in the strain maps [Fig. 1(c)]. Similar lines were previously observed in mist chemical vapor deposited α-Ga_2O_3 by Lee *et al.*, who ascribed them to anti-phase domain boundaries,[48,49] and in halide vapor phase epitaxy α-Ga_2O_3 by Myasoedov *et al.*, who assigned them to prismatic stacking faults with displacement vector $\mathbf{R} = \frac{1}{3}\langle 1\bar{1}00\rangle$.[33] In agreement with Myasoedov *et al.*, we observe that the threading dislocations in Fig. 1(a) are located on, or terminating in white lines.

Looking further into the structural properties of dislocations, Burgers circuits were drawn around 86 threading dislocations. All the Burgers circuits were open along $\mathbf{b_e} = \frac{1}{3}\langle 1\bar{1}00\rangle$, as illustrated in Fig. 2. Given that we here see a projection of the Burgers vector along the [0001] direction, this result implies that all the dislocations we observed are either partial edge dislocations (therefore with $\mathbf{b} = \frac{1}{3}\langle 1\bar{1}00\rangle$) or perfect mixed dislocations (with $\mathbf{b} = \frac{1}{3}\langle 1\bar{1}01\rangle$). The observation of partial edge dislocations implies that perfect edge dislocations have dissociated.

Looking into the sapphire (α-Al_2O_3) literature, $\mathbf{b} = \frac{1}{3}\langle 1\bar{1}01\rangle$ mixed dislocations, as well as dissociation of $\mathbf{b} = \frac{1}{3}\langle 11\bar{2}0\rangle$ and $\mathbf{b} = \langle 1\bar{1}00\rangle$ edge dislocations into $\mathbf{b} = \frac{1}{3}\langle 1\bar{1}00\rangle$ partials, have been reported at low-angle grain boundaries.[42] Given the high mosaicity of epitaxial α-Ga_2O_3 films,[45,50] the film contains a high density and wide variety of low-angle grain boundary configurations, implying that these three types of dislocations and partials could be possible here. In fact, while most reports on α-Ga_2O_3 concluded that edge dislocations formed the dominant category of dislocations, those works also observed dislocation contrast when $\mathbf{g} = 0006$, which implies that dislocations with screw component are expected.[15,34] In addition, Myasoedov *et al.* and Jinno *et al.* concluded that a significant proportion of the threading dislocation population exhibited a screw component.[19,33]

Figure 2 reveals that all three categories of dislocations coexist in the sample. While in several instances, the local density of dislocations is so high that it is not possible to identify with certainty if a dislocation fits in a given category, we could find examples shown in Fig. 2 where such categorization was clear.

Figure 2(a) shows an example of a perfect $\mathbf{b} = \frac{1}{3}\langle 11\bar{2}0\rangle$ edge dislocation that had dissociated into two partial dislocations with noncollinear $\mathbf{b} = \frac{1}{3}\langle 1\bar{1}00\rangle$ Burgers vectors, similar to what has been observed in Refs. 18 and 51. The two partial dislocations are ~2.7 nm apart and connected by a stacking fault (SF) contained roughly in the $\{11\bar{2}0\}$ prismatic plane. In this case, the dissociation reaction is

$$\frac{1}{3}\langle 11\bar{2}0\rangle \rightarrow \frac{1}{3}\langle 10\bar{1}0\rangle + \frac{1}{3}\langle 01\bar{1}0\rangle + SF. \quad (1)$$

Figure 2(b) shows a perfect $\mathbf{b} = \langle 1\bar{1}00\rangle$ edge dislocation that had dissociated into three partial dislocations with collinear $\mathbf{b} = \frac{1}{3}\langle 1\bar{1}00\rangle$ Burgers vectors. Here, the partial dislocations are ~3.4 and 3.8 nm apart and connected by a stacking fault contained roughly in the $\{11\bar{2}0\}$ prismatic plane. In this case, the dissociation reaction is

$$\langle 1\bar{1}00\rangle \rightarrow \frac{1}{3}\langle 1\bar{1}00\rangle + \frac{1}{3}\langle 1\bar{1}00\rangle + \frac{1}{3}\langle 1\bar{1}00\rangle + SF. \quad (2)$$

Dislocation dissociation can be rationalized energetically, as mentioned in introduction. The elastic energy of a dislocation scales with $\mathbf{b}^2$. Taking reaction (2) as an example, the perfect dislocation ($\mathbf{b_{perf}} = \langle 1\bar{1}00\rangle$) dissociates into three partial dislocations with Burgers vectors a third the length ($\mathbf{b_{part}} = \frac{1}{3}\langle 1\bar{1}00\rangle$). Dissociation leads to the combined elastic energy of the three partials being a third that of the perfect dislocation ($3 \times b_{part}^2 = 3 \times (\frac{b_{perf}}{3})^2 = \frac{1}{3}b_{perf}^2$). As long as the energy of the stacking fault connecting the partial dislocations is not excessive—and calculations in α-Al_2O_3 have shown that prismatic stacking faults are low energy in that material[52,53]—the dissociation reaction will be energetically favorable. We can use our observation of partial dislocation separation in Fig. 2 and crystal elastic parameters[54] to obtain an estimate of the stacking fault energy

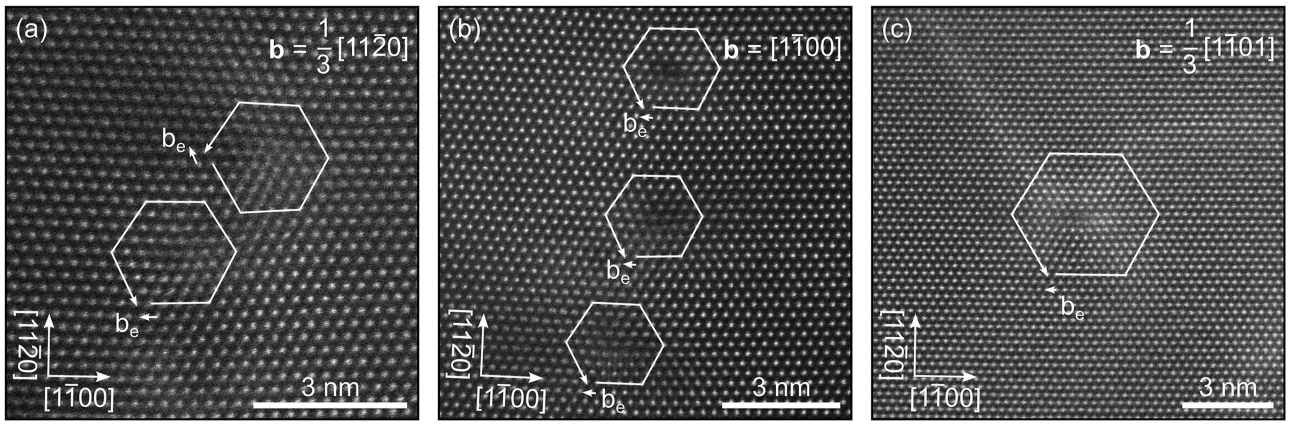

FIG. 2. Raw HAADF-STEM image depicting the different categories of dislocations observed through the sample: (a) edge $\mathbf{b} = \frac{1}{3}\langle 11\bar{2}0\rangle$ dislocation dissociated into two noncollinear $\mathbf{b} = \frac{1}{3}\langle 1\bar{1}00\rangle$ partial dislocations; (b) edge $\mathbf{b} = \langle 1\bar{1}00\rangle$ dislocation dissociated into three collinear $\mathbf{b} = \frac{1}{3}\langle 1\bar{1}00\rangle$ partial dislocations; and (c) mixed $\mathbf{b} = \frac{1}{3}\langle 1\bar{1}01\rangle$ dislocation, where only the edge component is seen in this projection.

and gauge if dissociation should be expected. Assuming that the repulsive force between the partials is balanced by the stacking fault attractive force, the stacking fault energy can be approximated by $\gamma_{SF} = \frac{Gb^2}{4\pi r}$ [55] (G: shear modulus; b: Burgers vector of partials; and r: separation of partials), which yields a stacking fault energy of the order of ~0.16–0.24 J.m^{-2}, which is low and well within the predicted prismatic faults energies in α-Al_2O_3 [52,53] (we note that since the elastic parameters are not well established in α-Ga_2O_3, a refined formulation of the stacking fault energy would not be meaningful).

Finally, Fig. 2(c) shows a perfect $\mathbf{b} = \frac{1}{3}\langle 1\bar{1}01\rangle$ mixed dislocation. This dislocation is >10 nm away from any other dislocation or free surface, which suggests that it cannot be issued from a dissociation mechanism as this would be energetically improbable.

Drawing statistics about the distance of each dislocation (or partial dislocation) to its nearest neighbor, we identify two distinct populations. A first category corresponds to dislocations spaced by <10 nm. These exhibit an average dislocation separation of 4.4 ± 0.3 nm and account for ~50% of the total dislocations. On the basis of dissociation energy balance, we therefore assign these to the partial dislocations. The second category corresponds to dislocations that can be considered as isolated, i.e., spaced by >10 nm, and accounts for the other 50% of the total population. We therefore associated that population to the perfect mixed dislocations. This result suggests that our sample exhibits an equivalent proportion of edge and mixed dislocations, in line with previous reports on α-Ga_2O_3 grown using other techniques.[19,33]

Finally, we turn our attention to the atomic arrangement of the core of the dislocations. Identifying the core structure of a dislocation is important as this underpins the electronic properties of the defect, and dislocations with identical Burgers vectors can, in fact, exhibit different core arrangements.[36,37] In our sample, 47 dislocations were sufficiently clear to allow unambiguous identification of their core structure—for a study of this nature, this is a statistically significant number of cores. Our analysis reveals that every dislocation exhibits the same 5-atom ring core structure, as illustrated in Fig. 3, irrespectively of whether the dislocation is edge partial or perfect mixed. We need to bear in mind that our micrographs only show the Ga cation columns in the crystal and that there may therefore be further differentiation of core configurations were the O columns visible. This result will, however, be extremely valuable to computational material scientists, allowing them to narrow their possible core exploration to uncover the accurate core structure and resulting density of states associated with the dislocations.

In conclusion, we presented a statistically meaningful investigation of threading dislocations in α-Ga_2O_3 using high-resolution HAADF-STEM. Seen end on, all 86 threading dislocations exhibit a projected Burgers vector $\mathbf{b_e} = \frac{1}{3}\langle 1\bar{1}00\rangle$. We find that the dislocations can be classified into perfect mixed dislocations ($\mathbf{b} = \frac{1}{3}\langle 1\bar{1}01\rangle$) and edge dislocations ($\mathbf{b} = \langle 1\bar{1}00\rangle$ and $\mathbf{b} = \frac{1}{3}\langle 11\bar{2}0\rangle$), which dissociate into combinations of $\mathbf{b} = \frac{1}{3}\langle 1\bar{1}00\rangle$ partials. High-resolution analysis of the core region of 47 dislocations identifies that all the dislocations exhibit a similar 5-atom core, when looking at the cation sites. We believe that this is the first investigation of its kind and magnitude in this material system, which will feed into important future simulation work to understand the electronic properties of dislocations in α-Ga_2O_3 as well as other epitaxial corundum-structured materials.

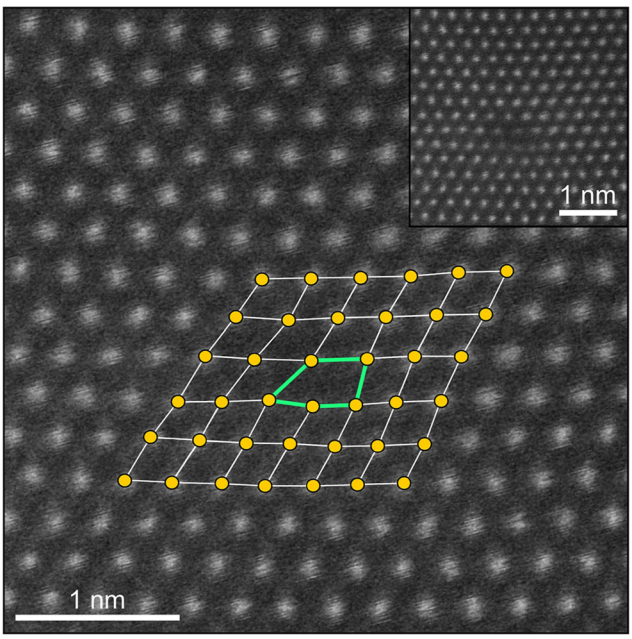

FIG. 3. Raw HAADF-STEM image of the atomic structure of a 5-atom dislocation core. In the inset, the same image without the Ga columns marking is shown.

The authors acknowledge the support from the Engineering and Physical Sciences Research Council (EPSRC Grant Nos. EP/M010589/1 and EP/K014471/1). The authors would like to thank Dr Giorgio Divitini (now at Istituto Italiano di Tecnologia, Genova, Italy) for his technical support on the TEM.

AUTHOR DECLARATIONS

Conflict of Interest

The authors have no conflicts to disclose.

Author Contributions

Ross Mullen: Data curation (equal); Formal analysis (equal); Writing – original draft (supporting); Writing – review & editing (supporting). **Joseph W. Roberts**: Conceptualization (supporting); Investigation (equal); Resources (equal); Writing – original draft (supporting); Writing – review & editing (supporting). **Paul R. Chalker**: Funding acquisition (equal); Resources (supporting); Supervision (supporting); Writing – original draft (supporting); Writing – review & editing (supporting). **Rachel A. Oliver**: Funding acquisition (equal); Resources (supporting); Supervision (supporting); Writing – original draft (supporting); Writing – review & editing (supporting). **Ben Hourahine**: Data curation (supporting); Formal analysis (supporting); Writing – original draft (supporting); Writing – review & editing (equal). **Fabien C.P. Massabuau**: Conceptualization (lead); Data curation (equal); Formal analysis

(lead); Funding acquisition (supporting); Writing – original draft (lead); Writing – review & editing (lead).

DATA AVAILABILITY

The data that support the findings of this study are openly available in PurePortal at (https://doi.org/10.15129/68379534-815b-448f-a7ca-a458750c944f).[56]

REFERENCES

[1] C. Xie, X.-T. Lu, X.-W. Tong, Z.-X. Zhang, F.-X. Liang, L. Liang, L.-B. Luo, and Y.-C. Wu, "Recent progress in solar-blind deep-ultraviolet photodetectors based on inorganic ultrawide bandgap semiconductors," Adv. Funct. Mater. **29**, 1806006 (2019).

[2] A. Green, J. Speck, G. Xing, P. Moens, F. Allerstam, K. Gumaelius, T. Neyer, A. Arias-Purdue, V. Mehrotra, A. Kuramata, K. Sasaki, S. Watanabe, K. Koshi, J. Blevins, O. Bierwagen, S. Krishnamoorthy, K. Leedy, A. Arehart, A. Neal, S. Mou, S. Ringel, A. Kumar, A. Sharma, K. Ghosh, U. Singisetti, W. Li, K. Chabak, K. Liddy, A. Islam, S. Rajan, S. Graham, S. Choi, Z. Cheng, and M. Higashiwaki, "β-gallium oxide power electronics," APL Mater. **10**, 029201 (2022).

[3] R. Roy, V. Hill, and E. Osborn, "Polymorphism of Ga_2O_3 and the system Ga_2O_3-h_2o," J. Am. Chem. Soc. **74**, 719 (1952).

[4] H. Playford, A. Hannon, E. Barney, and R. Walton, "Structures of uncharacterised polymorphs of gallium oxide from total neutron diffraction," Chem. - Eur. J. **19**, 2803–2813 (2013).

[5] I. Cora, F. Mezzadri, F. Boschi, M. Bosi, M. Caplovicova, G. Calestani, I. Dodony, B. Pecz, and R. Fornari, "The real structure of ϵ-Ga_2O_3 and its relation to κ-phase," CrystEngComm **19**, 1509 (2017).

[6] Z. Galazka, "Growth of bulk β-Ga_2O_3 single crystals by the Czochralski method," J. Appl. Phys. **131**, 031103 (2022).

[7] Y. Oshima and E. Ahmadi, "Progress and challenges in the development of ultra-wide bandgap semiconductor α-Ga_2O_3 toward realizing power device applications," Appl. Phys. Lett. **121**, 260501 (2022).

[8] A. Segura, L. Artús, R. Cuscó, R. Goldhahn, and M. Feneberg, "Band gap of corundumlike α-Ga_2O_3 determined by absorption and ellipsometry," Phys. Rev. Mater. **1**, 024604 (2017).

[9] H. Sun, K.-H. Li, C. G. T. Castanedo, S. Okur, G. Tompa, T. Salagaj, S. Lopatin, A. Genovese, and X. Li, "HCl flow-induced phase change of α-β-and ϵ-Ga_2O_3 films grown by mocvd," Cryst. Growth Des. **18**, 2370 (2018).

[10] J. Roberts, P. Chalker, B. Ding, R. Oliver, J. Gibbon, L. Jones, V. Dhanak, L. Phillips, J. Major, and F.-P. Massabuau, "Low temperature growth and optical properties of α-Ga_2O_3 deposited on sapphire by plasma enhanced atomic layer deposition," J. Cryst. Growth **528**, 125254 (2019).

[11] S. Fujita and K. Kaneko, "Epitaxial growth of corundum-structured wide band gap III-oxide semiconductor thin films," J. Cryst. Growth **401**, 588 (2014).

[12] D. Yang, B. Kim, T. Eom, Y. Park, and H. Jang, "Epitaxial growth of alpha gallium oxide thin films on sapphire substrates for electronic and optoelectronic devices: Progress and perspective," Electron. Mater. Lett. **18**, 113 (2022).

[13] B. Kunert, Y. Mols, M. Baryshniskova, N. Waldron, A. Schulze, and R. Langer, "How to control defect formation in monolithic iii/v hetero-epitaxy on (100) Si? A critical review on current approaches," Semicond. Sci. Technol. **33**, 093002 (2018).

[14] S. E. Bennett, "Dislocations and their reduction in GaN," Mater. Sci. Technol. **26**, 1017 (2010).

[15] K. Kaneko, H. Kawanowa, H. Ito, and S. Fujita, "Evaluation of misfit relaxation in α-Ga_2O_3 epitaxial growth on α-Al_2O_3 substrate," Jpn. J. Appl. Phys. **51**, 020201 (2012).

[16] Y. Oshima, K. Kawara, T. Shinohe, T. Hitora, M. Kasu, and S. Fujita, "Epitaxial lateral overgrowth of $\alpha\alpha$-Ga_2O_3 by halide vapor phase epitaxy," APL Mater. **7**, 022503 (2018).

[17] Y. Oshima, S. Yagyu, and T. Shinohe, "Visualization of threading dislocations in an α-Ga_2O_3 epilayer by HCl gas etching," J. Cryst. Growth **576**, 126387 (2021).

[18] H. Takane, S. Konishi, Y. Hayasaka, R. Ota, T. Wakamatsu, Y. Isobe, K. Kaneko, and K. Tanaka, "Structural characterization of threading dislocation in α-Ga_2O_3 thin films on c- and m-plane sapphire substrates," J. Appl. Phys. **136**, 025105 (2024).

[19] R. Jinno, T. Uchida, K. Kaneko, and S. Fujita, "Reduction in edge dislocation density in corundum-structured α-Ga_2O_3 layers on sapphire substrates with quasi-graded α-$(Al,Ga)_2O_3$ buffer layers," Appl. Phys. Express **9**, 071101 (2016).

[20] Y. Oshima, H. Ando, and T. Shinohe, "Reduction of dislocation density in α-Ga_2O_3 epilayers via rapid growth at low temperatures by halide vapor phase epitaxy," Appl. Phys. Express **16**, 065501 (2023).

[21] T. Sugahara, H. Sato, M. Hao, Y. Naoi, S. Kurai, S. Tottori *et al.*, "Direct evidence that dislocations are non-radiative recombination centers in GaN," Jpn. J. Appl. Phys. **37**, 398 (1998).

[22] D. Jung, R. Herrick, J. Norman, K. Turnlund, C. Jan, K. Feng, A. Gossard, and J. Bowers, "Impact of threading dislocation density on the lifetime of InAs quantum dot lasers on Si," Appl. Phys. Lett. **112**, 153507 (2018).

[23] P. Kozodoy, J. P. Ibbetson, H. Marchand, P. T. Fini, S. Keller, J. S. Speck, S. P. DenBaars, and U. K. Mishra, "Electrical characterization of GaN p-n junctions with and without threading dislocations," Appl. Phys. Lett. **73**, 975 (1998).

[24] M. Kasu, K. Hanada, T. Moribayashi, A. Hashiguchi, T. Oshima, T. Oishi, K. Koshi, K. Sasaki, A. Kuramata, and O. Ueda, "Relationship between crystal defects and leakage current in β-Ga_2O_3 Schottky barrier diodes," Jpn. J. Appl. Phys. **55**, 1202BB (2016).

[25] J. Yang, C. Fares, R. Elhassani, M. Xian, F. Ren, S. Pearton, M. Tadjer, and A. Kuramata, "Reverse breakdown in large area, field-plated, vertical β-Ga_2O_3 rectifiers," ECS J. Solid State Sci. Technol. **8**, Q3159 (2019).

[26] J. Cooke, P. Ranga, J. Jesenovec, J. McCloy, S. Krishnamoorthy, M. Scarpulla, and B. Sensale-Rodriguez, "Effect of extended defects on photoluminescence of gallium oxide and aluminum gallium oxide epitaxial films," Sci. Rep. **12**, 3243 (2022).

[27] H. Takane, H. Izumi, H. Hojo, T. Wakamatsu, K. Tanaka, and K. Kaneko, "Effect of dislocations and impurities on carrier transport in α-Ga_2O_3 on m-plane sapphire substrate," J. Mater. Res. **38**, 2645 (2023).

[28] S. Usami, Y. Ando, A. Tanaka, K. Nagamatsu, M. Deki, M. Kushimoto, S. Nitta, Y. Honda, H. Amano, Y. Sugawara, Y. Yao, and Y. Ishikawa, "Correlation between dislocations and leakage current of p-n diodes on a free-standing GaN substrate," Appl. Phys. Lett. **112**, 182106 (2018).

[29] B. Simpkins, E. T. Yu, P. Waltereit, and J. Speck, "Correlated scanning Kelvin probe and conductive atomic force microscopy studies of dislocations in gallium nitride," J. Appl. Phys. **94**, 1448 (2003).

[30] T. Hamachi, T. Tohei, Y. Hayashi, M. Imanishi, S. Usami, Y. Mori, and A. Sakai, "Comprehensive analysis of current leakage at individual screw and mixed threading dislocations in freestanding GaN substrates," Sci. Rep. **13**, 2436 (2023).

[31] F. C. P. Massabuau, P. Griffin, H. Springbett, Y. Liu, R. Kumar, T. Zhu, and R. Oliver, "Dislocations as channels for the fabrication of sub-surface porous GaN by electrochemical etching," APL Mater. **8**, 031115 (2020).

[32] F.-P. Massabuau, J. Bruckbauer, C. Trager-Cowan, and R. Oliver, Microscopy of defects in semiconductors (2019).

[33] A. Myasoedov, I. Pavlov, A. Pechnikov, S. Stepanov, and V. Nikolaev, "Planar defects in α-Ga_2O_3 thin films produced by HVPE," J. Appl. Phys. **135**, 125703 (2024).

[34] T. Ma, X. Chen, Y. Kuang, L. Li, J. Li, F. Kremer, F.-F. Ren, S. L. Gu, R. Zhang, Y. Zheng, H. Tan, C. Jagadish, and J. Ye, "On the origin of dislocation generation and annihilation in α-Ga_2O_3 epilayers on sapphire," Appl. Phys. Lett. **115**, 182101 (2019).

[35] M. Marezio and J. Remeika, "Bond lengths in the α-Ga_2O_3 structure and the high-pressure phase of $Ga_{2-x}Fe_xO_3$," J. Chem. Phys. **46**, 1862–1865 (1967).

[36] F. C. P. Massabuau, S. Rhode, M. Horton, T. Ohanlon, A. Kovàcs, M. Zielinski, M. Kappers, R. Dunin-Borkowski, C. Humphreys, and R. Oliver, "Dislocations in AlGaN: Core structure, atom segregation, and optical properties," Nano Lett. **17**, 4846 (2017).

[37] S. Rhode, M. Horton, S. Sahonta, M. Kappers, S. Haigh, T. Pennycook, C. McAleese, C. Humphreys, R. Dusane, and M. Moram, "Dislocation core structures in (0001) InGaN," J. Appl. Phys. **119**, 105301 (2016).

[38]P. Hirsch, J. Lozano, S. Rhode, M. Horton, M. Moram, S. Zhang, M. Kappers, C. Humphreys, A. Yasuhara, E. Okunishi, and P. Nellist, "The dissociation of the [**a** + **c**] dislocation in GaN," Philos. Mag. **93**, 3925 (2013).
[39]I. Arslan, A. Bleloch, E. Stach, and N. Browning, "Atomic and electronic structure of mixed and partial dislocations in GaN," Phys. Rev. Lett. **94**, 025504 (2005).
[40]H. Yang, J. Lozano, T. Pennycook, L. Jones, P. Hirsch, and P. Nellist, "Imaging screw dislocations at atomic resolution by aberration-corrected electron optical sectioning," Nat. Commun. **6**, 7266 (2015).
[41]M. Horton, S. Rhode, and M. Moram, "Structure and electronic properties of mixed (a+c) dislocation cores in GaN," J. Appl. Phys. **116**, 063710 (2014).
[42]E. Tochigi, A. Nakamura, N. Shibata, and Y. Ikuhara, "Dislocation structures in low-angle grain boundaries of α-Al_2O_3," Crystals **8**, 133 (2018).
[43]K. Tsuruta, E. Tochigi, Y. Kezuka, K. Takata, N. Shibata, A. Nakamura, and Y. Ikuhara, "Core structure and dissociation energetics of basal edge dislocation in α-Al_2O_3: A combined atomistic simulation and transmission electron microscopy analysis," Acta Mater. **65**, 76–84 (2014).
[44]A. Heuer, C. Jia, and K. Lagerlöf, "The core structure of basal dislocations in deformed sapphire (α-Al_2O_3)," Science **330**, 1227–1231 (2010).
[45]F.-P. Massabuau, J. Roberts, D. Nicol, P. Edwards, M. McLelland, G. Dallas, D. Hunter, E. Nicolson, J. Jarman, A. Kovács, R. Martin, R. Oliver, and P. Chalker, "Progress in atomic layer deposited α-Ga_2O_3 materials and solar-blind detectors," Proc. SPIE **11687**, 116870Q (2021).
[46]J. Roberts, J. Jarman, D. Johnstone, P. Midgley, P. Chalker, R. Oliver, and F.-P. Massabuau, "α-Ga_2O_3 grown by low temperature atomic layer deposition on sapphire," J. Cryst. Growth **487**, 23–27 (2018).
[47]M. Hytch, E. Snoeck, and R. Kilaas, "Quantitative measurement of displacement and strain fields from HREM micrographs," Ultramicroscopy **74**, 131 (1998).
[48]Y. Lee, B. Gil, D. Yang, M. Sheen, E. Yoon, Y. Park, H. Jang, S. Yoon, M. Kim, and Y. Kim, "Luminescence properties related anti-phase domain of α-Ga_2O_3," APL Mater. **11**, 051113 (2023).
[49]Y.-H. Lee, D. Yang, B. Gil, M.-H. Sheen, E. Yoon, Y. Park, H.-W. Jang, S. Yoon, M. Kim, and Y.-W. Kim, "Origin of extra diffraction spots for high crystalline alpha-Ga_2O_3," AIP Adv. **13**, 025148 (2023).
[50]Y. Oshima, E. Víllora, and K. Shimamura, "Halide vapor phase epitaxy of twin-free α-Ga_2O_3 on sapphire (0001) substrates," Appl. Phys. Express **8**, 055501 (2015).
[51]A. Myasoedov, I. Pavlov, A. Pechnikov, S. Stepanov, and V. Nikolaev, "TEM study of the defect structure of α-Ga_2O_3 layers grown by HVPE," St. Petersburg State Polytech. Univ. J. Phys. Math. **16**, 16 (2023).
[52]P. Kenway, "Calculated stacking-fault energies in α-A_2O_3," Philos. Mag. B **68**, 171 (1993).
[53]M. Jhon, A. Glaeser, and D. Chrzan, "Computational study of stacking faults in sapphire using total energy methods," Phys. Rev. B **71**, 214101 (2005).
[54]K. Lion, P. Pavone, and C. Draxl, "Elastic stability of Ga_2O_3: Addressing the β to α phase transition from first principles," Phys. Rev. Mater. **6**, 013601 (2022).
[55]D. Hull and D. Bacon, *Introduction to Dislocations* (Butterworth-Heinemann, 2011).
[56]Dataset: R. Mullen, J. W. Roberts, P. R. Chalker, R. A. Oliver, B. Hourahine, and F. C. P. Massabuau (2024). "Atomic scale observation of threading dislocations in α-Ga2O3," PurePortal. https://doi.org/10.15129/68379534-815b-448f-a7ca-a458750c944f.